

Article ID: 1007-4627(2016)02-0235-07

Alpha Decay as a Probe of the Structure of Neutron-deficient Nuclei Around $Z = 82$

QI Chong(齐冲)

(Department of Physics, KTH Royal Institute of Technology, Stockholm SE-10691, Sweden)

Abstract: In this contribution I would like to review briefly our recent studies on nuclear α formation probabilities in heavy nuclei and their indication on the underlying structure of the nuclei involved. In particular, I will show that the empirical α -formation probabilities, which can be extracted from experimental half-lives, exhibit a rather smooth function with changing proton or neutron numbers. This allows us to distinguish the role played by pairing collectivity in the clustering process. The sudden hindrance of the clustering of the nucleons around the $N = 126$ shell closure is due to the fact that the configuration space does not allow a proper manifestation of the pairing collectivity. The influence of the $Z = 82$ shell closure on the α formation properties will also be discussed. Moreover, we have evaluated the α -decay fine structure to excited 0^+ states in Hg and Rn isotopes as well as the α -decay from the excited 0^+ states in the mother nucleus. It is thus found that the α decay is sensitive to the mixture of configurations corresponding to different nuclear shapes.

Key words: α decay; α formation probability; shell effect; neutron-deficient nuclei; pairing correlation

CLC number: O571.2 **Document code:** A **DOI:** 10.11804/NuclPhysRev.33.02.235

1 Introduction

There has been a constant attention to α decay studies in nuclear physics due to the relative simplicity of its experimental investigation and to the wealth of spectroscopic information it provides (see, e.g., Refs. [1-2]). The α -decay process is important for understanding crucial problems including cluster decay (emission of nuclei heavier than α particle), stellar nucleosynthesis as well as the synthesis and decay of super-heavy elements.

The gross features of $\Delta L = 0$ α transitions (e.g. between the $I^\pi = 0^+$ ground states of even-even nuclei) are expressed by the Geiger-Nuttall (GN) law^[3]. It linearly relates the logarithm of the partial half-life $T_{1/2}$ with the inverse square root of the Q value. The GN law has been verified in long isotopic chains and strong deviations are rarely observed. The law is well understood within the Gamow theory as due to quantum-mechanical “tunneling” of a “pre-formed” α particle through spherical barrier^[4-5]. Now we realize that the α decay can be properly described as a two-step process, which involves the preformation of an α particle at the nuclear surface, followed by its penetration through the barrier.

Still one may wonder why effective approaches based on the Gamow theory have been so successful. The reason is that the α -particle formation probability usually varies from nucleus to nucleus much less than the penetrability. In the logarithm scale of the GN law the differences in the formation probabilities are usually small fluctuations along the straight lines it predicted. What is missing in this picture is the possibility that the cluster is not “pre-formed” in the mother nucleus. In other words, one has to evaluate the probability that the cluster indeed is present on the nuclear surface. The greatest challenge has been to describe properly how the α particle is formed inside the nucleus from four independent particles^[6-7] and how the clustering is influenced by the residual interactions between like particles as well as those between the protons and neutrons. This can be done within the framework of the microscopic nuclear structure models including the shell model configuration interaction approach.

2 Microscopic description of α decay and the α preformation probability

We firstly go through briefly the microscopic R -

Received date: 31 Aug. 2015;

Foundation item: Swedish Research Council (VR)(621-2012-3805, 621-2013-4323); Göran Gustafsson Foundation

Biography: QI Chong (1983–), male, Zibo, Shandong, Ph.D./Prof., working on theoretical nuclear physics;

E-mail address: chongq@kth.se.

matrix description of the α decay^[8] and the derivations of Refs. [9–11] where a generalization of the GN law was found. According to Ref. [8], the α -decay half-life can be written as

$$T_{1/2} = \frac{\ln 2}{\nu} \left| \frac{H_l^+(\chi, \rho)}{RF(R)} \right|^2, \quad (1)$$

where ν is the velocity of the emitted α particle with angular momentum l . R is a distance chosen around the nuclear surface where the internal wave function is matched with the outgoing cluster wave function. H^+ is the Coulomb-Hankel function with $\rho = \mu\nu R/\hbar$ and $\chi = 4Ze^2/\hbar\nu$. μ is the reduced mass and Z is the charge number of the daughter nucleus. The quantity $F(R)$ is the formation amplitude of the α cluster at distance R . Introducing the quantities $\chi' = 2Z\sqrt{A_{\alpha d}/Q_{\alpha}}$ and $\rho' = \sqrt{2A_{\alpha d}Z(A_d^{1/3} + 4^{1/3})}$ where $A_{\alpha d} = 4A_d/(4 + A_d)$ and imposing the condition of the half life being independent on R , one gets^[9]

$$\log T_{1/2} = a\chi' + b\rho' + c = 2aZ/\sqrt{A_{\alpha d}Q_{\alpha}^{-1/2}} + b\sqrt{2A_{\alpha d}Z(A_d^{1/3} + 4^{1/3})} + c, \quad (2)$$

where a , b and c are constant parameters which only depend upon local variations of the formation probability. They can be determined by fitting to experimental data^[9]. This generalization holds well for all isotopic chains and all cluster radioactivities.

The reason why these parameters are practically constant is that, when going from one isotope to another, the α -particle formation probability usually varies much less than the penetrability. In other words, it is a consequence of the smooth variation in the nuclear structure that is often found when going from a nucleus to its neighbors. This is also the reason why, for example, the BCS approximation works so well in many regions of nuclei.

2.1 Relation to the GN law

According to the GN law^[3], the α decay partial half-life $T_{1/2}$ is given by,

$$\log_{10} T_{1/2} = A(Z)Q_{\alpha}^{-1/2} + B(Z), \quad (3)$$

where $A(Z)$ and $B(Z)$ are the coefficients which are determined for each isotopic chain. A correspondence between the coefficients $A(Z)$ and $B(Z)$ and the expressions $a\chi'$ and $b\rho' + c$ respectively can be deduced. $A(Z)$ models the tunneling process as well as the relatively small variations in the structure of the neighboring nuclei. The parameter $B(Z)$ takes into account the clusterization of the α -particle in the mother nucleus. By this representation a linear dependency of

$A(Z)$ upon Z is expected. $B(Z)$ are negative since both terms b and c are negative^[9]. The linear dependence upon Z of $B(Z)$ seems to be in conflict with the $Z^{1/2}$ dependence of the term ρ' . However for nuclei with known α -decay half-lives, ρ' is practically a linear function of Z .

2.2 The α formation amplitude

Eq. (1) is valid for the decays of all clusters from proton to heavy particles^[6–7, 12] decay width is obtained by assuming a two-step process: In the first step the formation of the cluster and its motion in the daughter nuclear surface is established. Then the cluster, with the formation amplitude and wave function thus determined, is assumed to penetrate through the centrifugal and Coulomb barriers. The amplitude of the wave function in the internal region is the formation amplitude, *i.e.*,

$$F(R) = \int d\mathbf{R} d\xi_d d\xi_c [\Psi(\xi_d)\phi(\xi_c)Y_l(\mathbf{R})]_{J_m M_m}^* \times \Psi_m(\xi_d, \xi_c, \mathbf{R}), \quad (4)$$

where d , c and m label the daughter, emitting cluster and mother nuclei, respectively. Ψ are the intrinsic wave functions and ξ the corresponding intrinsic coordinates. $\phi(\xi_c)$ is a Gaussian function of the relative coordinates of the nucleons that constitute the cluster. The important feature that we used in the derivation of the universal decay law^[9–10] is that the decay width is independent upon the matching radius R .

The formation amplitude $F(R)$ can be extracted from the experimental half-lives by

$$\log |RF(R)| = \frac{1}{2} \log \left[\frac{\ln 2}{\nu} |H_0^+(\chi, \rho)|^2 \right] - \frac{1}{2} \log T_{1/2}^{\text{Expt.}}. \quad (5)$$

In the first applications of the shell model to the description of the mother nucleus of α decay only one configuration was used. The theoretical decay rates were smaller than the corresponding experimental values by 4 ~ 5 orders of magnitude^[13]. We now understand that, since the matching radius R has to be chosen at a distance beyond the range of the nuclear force and Pauli exchanges, the formation amplitude would have required shell models for the mother and daughter nuclei with large bases. With the very limited shell-model spaces used at that time, the region of prominent four-particle correlation was not reached. Another problem with those early microscopic calculations was that the residual nucleon-nucleon interaction was not known well enough. Soon after the pairing interaction had been adapted to nuclei^[14–15], it was also applied to α decay^[16–17]. It was then found with great relief that the pairing interaction, which links many

shell-model configurations together, highly enhances the calculated α -decay width. Although the calculated widths were still too small by orders of magnitude, it was clear that this discrepancy had to be attributed to the small shell-model spaces allowed by the computing facilities at that time.

The fundamental role of configuration mixing was confirmed by actual large-scale calculations^[18–19] for nuclei around shell closures. The physics behind the enhancement induced by configuration mixing is that, with the participation of high-lying configurations, the pairing interaction clusters the two neutrons and the two protons on the nuclear surface.

2.3 The formation probability and effective quantities

The formation amplitude $F(R)$ can be extracted from the experimental half-lives data and is a model-independent quantity. We suggest that it is the formation amplitude or formation probability that should be calculated and compared with those extracted from experimental data. A simple Fortran code is available to extract the formation probability from experimental decay half-lives^[20]. On the other hand, the so-called preformation factor, given as the difference between the calculation and the experimental datum, is often introduced in many effective models. This preformation factor depends strongly on the shape of the effective potential employed^[21]. The reduced width introduced in Ref. [22] is also a similar effective quantity that depends on the effective optical potential. Here we show how the two-step mechanism is manifested in effective models where the α formation process is not explicitly taken into account. In the semiclassical approach, the decay width is given as^[21, 23–24]

$$\Gamma = S_{\text{eff}} F_{\text{eff}} \exp \left[-2 \int_{R_1}^{R_2} k(r) dr \right], \quad (6)$$

where S_{eff} is the effective preformation factor, F_{eff} a proper normalization factor^[21] and R_1 and R_2 the classical turning points. Since the radius R should satisfy the relation of $R_1 < R < R_2$, we have

$$\Gamma = S_{\text{eff}} F_{\text{eff}} \exp \left[-2 \int_{R_1}^R k(r) dr \right] P(R), \quad (7)$$

where $k(r) = \sqrt{2\mu|Q_c - V(r)|}/\hbar$ with $V(r)$ being the effective potential between the cluster and the daughter nucleus. For convenience we define a penetration factor P that is given as

$$P(R) = \exp \left\{ -2 \int_R^{R_2} \sqrt{\frac{2\mu}{\hbar^2} |V_C(r) - Q_c|} dr \right\}, \quad (8)$$

where $V_C(r) = Z_d Z_c e^2 / r$ is the Coulomb potential. Above equation can be integrated exactly, giving,

$$P = \exp \left\{ -2 Z_c Z_d e^2 \sqrt{\frac{2\mu}{Q_c \hbar^2}} \times \left[\arccos \sqrt{\frac{R}{R_2}} - \sqrt{\frac{R}{R_2}} \sqrt{1 - \frac{R}{R_2}} \right] \right\}.$$

Inserting $\chi = Z_c Z_d e^2 \hbar \sqrt{2\mu/Q_c}$, $R_2 = Z_c Z_d e^2 / Q_c$ and

$$\frac{R}{R_2} = \frac{\rho}{\chi} = \frac{Q_c}{V_C(R)}, \quad (9)$$

one immediately recognized that the penetration factor in the effective approach is related to the Coulomb function as,

$$P = \frac{[H_0^+(\chi, \rho)]^{-2}}{\tan \beta} = \exp[-2\chi(\beta - \sin \beta \cos \beta)]. \quad (10)$$

Similarly, the decay width in the fission model can be given as (see, *e.g.*, Ref. [25]),

$$\Gamma = F_{\text{f}} \exp \left[\frac{-2}{\hbar} \int_{R_{\text{f}}}^{R_2} \sqrt{2B(r)E(r)} dr \right] = F_{\text{f}} \exp \left[\frac{-2}{\hbar} \int_{R_{\text{f}}}^R \sqrt{2B(r)E(r)} dr \right] P(R), \quad (11)$$

where F_{f} is the frequency of assaults, $B(r)$ the nuclear inertia, $E(r)$ the deformation energy from which the Q value has been subtracted. Above relation is hold since we should have $B(r) = \mu$ and $E(r) = V_C(r) - Q_c$ beyond the radius R .

Since one has $\Gamma = \hbar \nu (RF(R)/H_0^+(\chi, \rho))^2$, the relation between the formation probability and the effective preformation factor is obvious, from which one can understand that the preformation factor thus introduced is not an observable. It strongly depends on the choice of the effective potential.

2.4 The pairing gap and di-nucleon correlation

Within the BCS approach the two-particle formation amplitude is proportional to $\sum_k u_k v_k$ where u_k and v_k are the standard occupation numbers. To this one adds the overlap of the corresponding proton and neutron radial functions with the α -particle intrinsic wave function on the nuclear surface. On the other hand, the corresponding pairing gap is given by,

$$\Delta = G \sum_k u_k v_k, \quad (12)$$

where G is the pairing strength. We thus find that the α formation amplitude is proportional to the product of the proton and the neutron pairing gaps. To probe this conjecture one can compare the formation probabilities extracted from the experimental half-lives to

the corresponding pairing gaps. The latter can readily be obtained from the experimental binding energies by using the three-point formula as^[26–28],

$$\Delta_n(Z, N) = \frac{1}{2} [B(Z, N) + B(Z, N - 2) - 2B(Z, N - 1)]. \quad (13)$$

Recent systematic studies on the neutron odd-even staggering pairing gaps are presented in Ref. [26–27, 29] with experimental data from Ref. [30]. A large-scale shell model calculation on the odd-even staggering in Pb isotopes is presented in Ref. [31]. As examples, we presented in Fig. 1 our calculations

with the Skyrme-Hartree-Fock-Bogoliubov (HFB) and large-scale shell model approaches on the odd-even staggering in Pb isotopes. The HFB calculations are done with three different density-dependent zero-range pairing interactions, namely the volume pairing, mixed pairing and the surface pairing interaction. The results marked as “LCS” and “ave” in the figure correspond to the lowest canonical state pairing gap and the average pairing gap respectively. The shell-model calculations are done with an optimized effective two-body interaction. More details could be found in Refs. Ref. [26–27, 29].

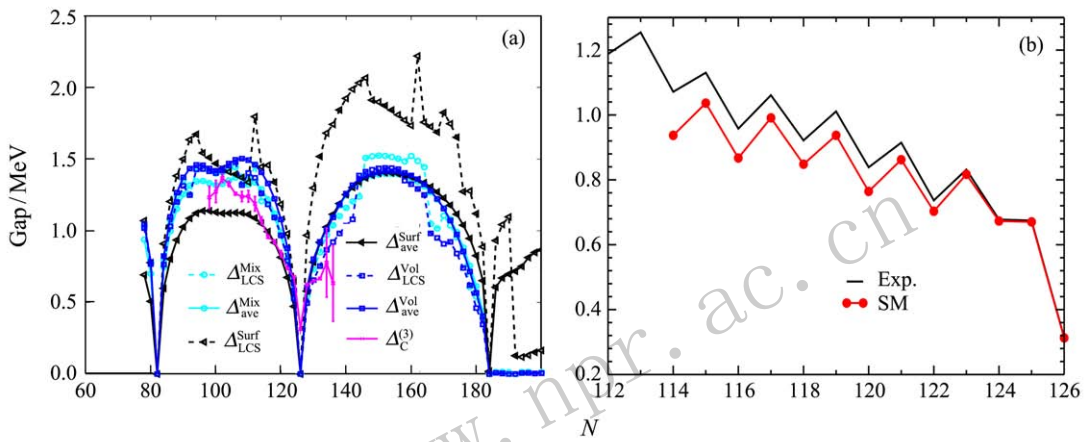


Fig. 1 (color online) (a) Experimental pairing gaps as a function of the neutron number N and those predicted by the HFB theory with different pairing interactions; (b) Large-scale shell model (SM) calculations on the pairing gaps of $N < 126$ Pb isotopes.

3 Systematic studies on the α decay properties in nuclei around $Z = 82$

Almost all observed proton-rich exotic nuclei starting from $A \sim 150$ have α radioactivities. The spontaneous emission of charged fragments heavier than the α particle is known as cluster radioactivity. Heavy-cluster decays have been established experimentally in trans-lead nuclei decaying into daughters around the doubly magic nucleus ^{208}Pb . A second island of cluster radioactivities was predicted in trans-tin nuclei decaying into daughters close to ^{100}Sn . Using the universal decay law it is straightforward to evaluate the half-lives of all cluster emitters throughout the nuclear chart if reliable values of the binding energies (*i.e.*, of the cluster Q -values) can be obtained.

We found that although the calculation reproduces nicely most available experimental α decay data, as expected, there is a case where it fails by a large factor. This corresponds to the α decays of nuclei with neutron numbers equal to or just below $N = 126$ ^[32–33], as can be seen from the left panel of Fig. 2 where we

plotted the discrepancy between experimental and calculated α half-lives. The reason for this large discrepancy is that, as indicated in the right panel of Fig. 2, the α formation amplitudes in $N \leq 126$ nuclei are much smaller than the average quantity predicted. The α decay of the nucleus ^{210}Po shows the most significant hindrance. We found that the formation amplitude in ^{210}Po is hindered with respect to the one in ^{212}Po due to the hole character of the neutron states in the first case. This is a manifestation of the mechanism that induces clusterization, which is favored by the presence of high-lying configurations. Such configurations are more accessible in the neutron-particle case of ^{212}Po than in the neutron-hole case of ^{210}Po ^[32–33]. This is a general feature in nuclei where neutrons and protons occupy different low-lying major shells.

We studied the origin and physical meaning of the coefficients $A(Z)$ and $B(Z)$ in the GN law. These coefficients are determined from experimental data and show a linear dependence upon Z . The need for a different linear Z dependence of the GN coefficients A and B in four different regions of the nuclear chart has

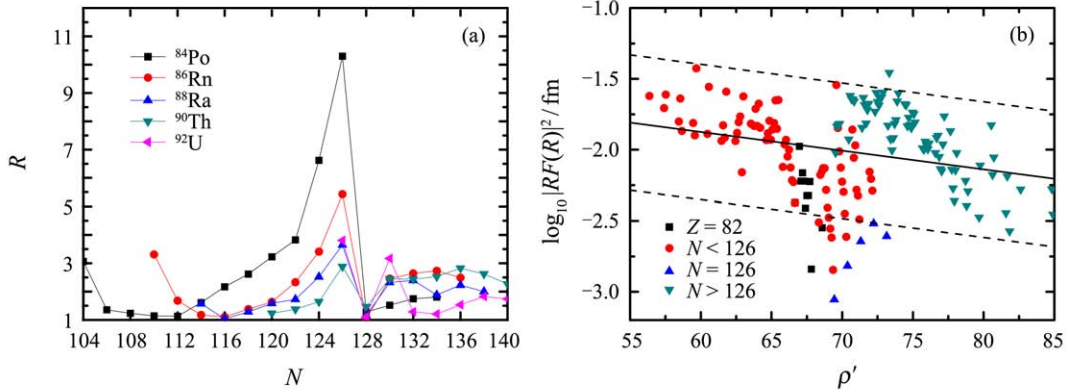


Fig. 2 (color online) (a) Discrepancy between experimental decay half-lives and UDL calculations as a function of the neutron number of the mother nucleus N ; (b) $\log_{10}|RF(R)|^2$ as a function of ρ' .

been addressed recently in Ref. [34]. A generic form for the evolution of the α formation probabilities was proposed in Refs. [29, 34] and is illustrated in Fig. 3.

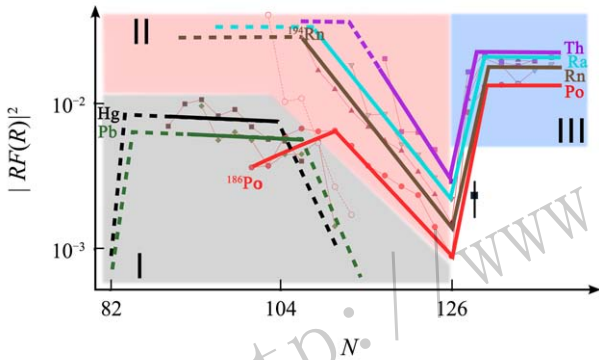


Fig. 3 (color online) A generic form of the α formation probability.

As can be seen from the figure, the experimental α formation probabilities of most known α emitters in nuclei with $N \leq 126$, $Z \leq 82$ and those with $N > 126$, $Z > 82$ are nearly constant as a function of neutron number (or more exactly, weakly linearly dependent on ρ' , as seen in Fig. 1 of Ref. [32]). For those nuclei, the GN law is indeed expected to be valid and $A(Z)$ and $B(Z)$ follow a linear behavior as a function of Z .

Approaching the $N = 126$ shell closure from below, a strong and exponential decrease of the formation probability is observed^[29]. This behavior has a fundamental influence on the prediction of the GN law on α decay half-lives^[34]. It is striking that in spite of a variation of $|RF_{\alpha}(R)|^2$ over one order of magnitude, the GN law and the $A(Z)$ and $B(Z)$ linear dependence upon Z are still valid. This is a consequence of the specific dependence of the $|RF_{\alpha}(R)|^2$ on Q_{α} . The Q_{α} (as well as $Q_{\alpha}^{-1/2}$) values also exhibit a quasi linear pattern as a function of neutron number when approaching the $N = 126$ shell closure. Therefore $\log_{10}|RF(R)|^2$ and

thus $\log_{10}(T_{1/2})$ will still depend linearly on $Q_{\alpha}^{-1/2}$. The formation probabilities in nuclei with $N \leq 126$, $Z > 82$ show a similar linearly decreasing behavior of $\log_{10}|RF(R)|^2$ as a function of $Q_{\alpha}^{-1/2}$, however with different slopes. As a result, the GN law remains valid for isotopic chains in that region, but the corresponding values of A and B will increase with Z .

For the polonium isotopic chain with $N < 126$, the linear behavior of $\log_{10}|RF(R)|^2$ breaks down below ^{196}Po . This explains why the GN law is broken in the light polonium isotopes. This violation of the GN law is induced by the strong suppression of the α formation probability^[34]. This is due to the fact that the deformations and configurations of the ground states of the lightest α -decaying neutron-deficient polonium isotopes ($A < 196$) are very different from those of the daughter lead isotopes^[35–36].

The different values of the α formation probability in different regions can be understood as due to the available j orbitals and a difference in the clustering properties of the nucleons in the α particle. Clustering of the two protons and two neutrons leading to the α -particle formation proceeds through high-lying empty single particle configurations. It would therefore be very interesting to extend the experimental knowledge towards more neutron deficient radon, radium and thorium isotopes. In Ref. [29] one notes a striking similarity between the tendency of the pairing gaps in this figure with the α -particle formation probabilities. As examples, the empirical neutron pairing gaps for Pb isotopes are plotted in Fig. 3 and compared with those given by different density functional calculations^[26]. This similarity makes it possible to draw conclusions on the tendencies of the formation probabilities. The near constant value of $|RF_c(R)|^2$ for neutron numbers $N \leq 114$ is due to the influence of the $i_{13/2}$ and other high- j orbitals including $h_{9/2}$ and

$1f_{7/2}$ at the lower end of the major $N = 82$ to 126 shell. As these highly degenerate shells are being filled the pairing gap, Eq. (13), and the formation probability, should remain constant. A quite sharp decrease of formation probability and pairing gap happens as soon as the low- j orbitals like $2p_{3/2}$, $1f_{7/2}$ and $2p_{1/2}$ start to be filled between $N = 114$ and $N = 126$. Finally, when we reach $N = 126$, the pairing reaches its lowest value. As the neutron pairing gap Δ_n varies smoothly, the two-neutron clustering in the mercury, lead, polonium, radon and radium isotopes are all of a similar character. Those with neutron number between 102 and 110, show an enhanced α formation probability for the radon, radium and thorium isotopes compared to mercury and lead. This behavior is a clear manifestation of crossing the $Z = 82$ shell.

In Ref. [37], we analyzed the α -decay fine structure to excited 0^+ states in Hg and Rn isotopes. We described these states as the deformation minima as provided by a deformed Woods-Saxon plus pairing approach. We estimated the hindrance factor of excited states relative to ground states by using the corresponding α -decay formation amplitudes. It is seen that the investigation of α -decay fine structure is a very powerful tool to probe deformations and shape coexistence in nuclei. A systematic calculation on the shape coexistence over the whole nuclear chart within the same structure model is done recently in Ref. [38].

Moreover, it might be interesting to pose a question whether the formation probabilities of the neutron-deficient isotopes with $N \sim Z$ are larger compared to their neutron rich counterparts. If it is indeed correct, that would mean that the cluster formation increases when protons and neutrons occupy the same shells^[39–41]. Refs. [39–40] compared the α -decay reduced widths for Xe and Te nuclei with that of ^{212}Po and neighboring Po isotopes and an enhancement by a factor of $2 \sim 3$ is seen. It is noted that the $|RF(R)|^2$ value of ^{194}Rn is larger by a similar factor compared to the $|RF(R)|^2$ of the textbook α -decay isotope ^{212}Po . This faster α decay would change the borderline of accessible neutron deficient α -decaying nuclei and might be a important question and motivation for further experimental work^[41].

4 Summary

We presented briefly the microscopic studies of the α decay. An abrupt change in α formation amplitudes is noted around the $N = 126$ shell closure. It is related to the suppression of pairing collectivity around shell closures. A possible influence of the $Z = 82$ shell closure may also be seen. α decay can serve as a powerful

probe for nuclear structure in neutron-deficient nuclei. It will also help clarify the influence of the neutron-proton correlation with the observation of α decay in $N \sim Z$ nuclei.

Acknowledgements I thank A. N. Andreyev, D.S. Delion, M. Huyse, R. J. Liotta, P. Van Duppen, R. Wyss for collaborations on the present subject and X.D. Tang and the procon2015 local organizers for their kind support of my stay. This work was supported by the Swedish Research Council (VR) under grant Nos. 621-2012-3805, 621-2013-4323 and the Göran Gustafsson foundation. I also thank the Swedish National Infrastructure for Computing (SNIC) at NSC in Linköping and PDC at KTH, Stockholm for computational support.

References:

- [1] MA L, ZHANG Z Y, GAN Z G, *et al.* Phys Rev C, 2015, **91**: 051302.
- [2] ZHANG Z Y, GAN Z G, MA L, *et al.* Phys Rev C, 2014, **89**: 014308.
- [3] GEIGER H, NUTTALL J M. Philos Mag, 1911, **22**: 613; GEIGER H. Z Phys, 1922, **8**: 45.
- [4] GAMOW G. Z Phys, 1929, **52**: 510.
- [5] CONDON E U, GURNEY R W. Nature (London), 1928, **122**: 438; GURNEY R W, CONDON E U. Phys Rev, 1929, **33**: 127.
- [6] LOVAS R G, LIOTTA R J, INSOLIA A, *et al.* Phys Rep, 1998, **294**: 265.
- [7] DELION D S. Theory of Particle and Cluster Emission[M]. Berlin: SpringerVerlag, 2010.
- [8] THOMAS R G. Prog Theor Phys, 1954, **12**: 253.
- [9] QI C, XU F R, LIOTTA R J, *et al.* Phys Rev Lett, 2009, **103**: 072501.
- [10] QI C, XU F R, LIOTT R J, *et al.* Phys Rev C, 2009, **80**: 044326.
- [11] QI C, LIOTTA R J, WYSS R. J Phys: Conf Ser, 2012, **381**: 012131.
- [12] QI C, DELION D S, LIOTTA R J, *et al.* Phys Rev C, 2012, **85**: 011303(R).
- [13] MANG H J. Phys Rev, 1960, **119**: 1069.
- [14] BOHR A, MOTTELSON B R, PINES D. Phys Rev, 1958, **110**: 936.
- [15] BELYAEV S T. Danske Videnskab Kgl Selskab Mat-Fys Medd, 1958, **31**: 11.
- [16] MANG H J, RASMUSSEN J O. Kgl Danske Videnskab Selskab Mat-Fys Skifter, 1962, **2**: 3.
- [17] SOLOVIEV V G. Phys Lett, 1962, **1**: 202.
- [18] TONOZUKA I, ARIMA A. Nucl Phys A, 1979, **323**: 45.
- [19] JANOUCHE F A, LIOTTA R J. Phys Lett B, 1979, **82**: 329.
- [20] QI C, unpublished, available upon request.
- [21] BUCK B, MERCHANT A C, PEREZ S M. Phys Rev Lett, 1990, **65**: 2975.
- [22] RASMUSSEN J O. Phys Rev, 1969, **113**: 1593.

- [23] ZHANG H F, DONG J M, ROYER G, *et al.* Phys Rev C, 2009, **80**: 037307.
- [24] QIAN Y, REN Z. Phys Rev C, 2014, **90**: 064308.
- [25] POENARU D N, NAGAME Y, GHERGHESCU R A, *et al.* Phys Rev C, 2002, **65**: 054308.
- [26] CHANGIZI S A, QI C. Phys Rev C, 2015, **91**: 024305.
- [27] CHANGIZI S A, QI C, WYSS R. Nucl Phys A, 2015, **940**: 210; CHANGIZI S A, QI C. Nucl Phys A, 2015, **951**: 97.
- [28] QI C. Phys Lett B, 2012, **717**: 436.
- [29] ANDREYEV A N, HUYSE M, Van DUPPEN P, *et al.* Phys Rev Lett, 2013, **110**: 242502.
- [30] AUDI G, BERSILLON O, BLACHOT J, *et al.* Nucl Phys A, 2003, **729**: 3; AUDI G, KONDEV F G, WANG M, *et al.* Chin Phys C, 2012, **36**: 1157; WANG M, AUDI G, WAPSTRA A, *et al.* Chin Phys C, 2012, **36**: 1603.
- [31] QI C, JIA L Y, FU G J. Phys Rev C, 2016, **94**: 014312.
- [32] QI C, ANDREYEV A N, HUYSE M, *et al.* Phys Rev C, 2010, **81**: 064319; QI C, ANDREYEV A N, HUYSE M, *et al.* AIP Conf Proc, 2011, **1377**: 296.
- [33] QI C, LIOTTA R J, WYSS R. J Phys: Conf Ser, 2011, **321**: 012048.
- [34] QI C, ANDREYEV A N, HUYSE M, *et al.* Phys Lett B, 2014, **734**: 203 ; QI C. Reviews in Physics, 2016, **1**: 77.
- [35] ANDREYEV A N, HUYSE M, Van DUPPEN P, *et al.* Phys Rev Lett, 1999, **82**: 1819.
- [36] KARLGREN D, LIOTTA R J, WYSS R, *et al.* Phys Rev C, 2006, **73**: 064304.
- [37] DELION D S, LIOTTA R J, QI C, *et al.* Phys Rev C, 2014, **90**: 061303.
- [38] WU Z Y, QI C, WYSS R, *et al.* Phys Rev C, 2015, **92**: 024306.
- [39] LIDDICK S N, GRZYWACZ R, MAZZOCCHI C, *et al.* Phys Rev Lett, 2006, **97**:082501.
- [40] LIDDICK S N, GRZYWACZ R, MAZZOCCHI C, *et al.* Eur Phys J: Special Topics, 2007, **150**: 131.
- [41] SEWERYNIAK D, STAROSTA K, DAVIDS C N, *et al.* Phys Rev C, 2006, **73**: 061301; SEWERYNIAK D, the same issue.

<http://www.npr.ac.cn>